Spatial Modulation-Based Techniques for Backscatter Communication Systems

Eleni Goudeli, *Graduate Student Member, IEEE*, Constantinos Psomas, *Senior Member, IEEE*, and Ioannis Krikidis, *Fellow, IEEE*

***Abstract*—A vision of digital and connected world is now a global strategy for 5G internet of things (IoT), targeting for high speed communication services with more capacity, lower latency, increased reliability and availability. In this paper, we assess the added value of backscatter communication in 5G IoT technology, by studying spatial modulation-based techniques, applied over a traditional multiple antenna backscatter communication system. Particularly, with backscatter we fulfill the need for wireless self-powered devices, as one of the main characteristics of 5G IoT. Furthermore, with the use of multiple antennas, we apply sophisticated techniques that enhance the overall efficiency of the backscatter communication system. Initially, we study generalized spatial modulation (GSM) and its special case of spatial modulation (SM), exploiting the antenna index as an additional source of information. With this technique, enhanced performance in terms of symbol error rate (SER) and spectral efficiency, is provided. In addition, we expand GSM in time domain, by applying Alamouti coding scheme (GSMA) in two out of the multiple available antennas. In this way, we further enhance the performance and succeed transmit diversity. Finally, analytical expressions regarding the pairwise error probability are derived and presented, while a diversity analysis is carried out for the proposed techniques. Simulation results along with theoretical bounds are provided, validating the enhanced performance of our study.**

***Index Terms*—Backscatter communications, multiple antennas, generalized spatial modulation, Alamouti space time code, diversity.**

I. Introduction

The Internet of Things (IoT) continues its brisk and steady rise, while many research directions that started in previous years continue or even accelerate for the foreseeable future [1]. The growing scope of IoT technology has attracted the academia and the industrial interest, while is rapidly adopted and developed, targeting a massive number of connected sensors, rendering devices and actuators with stringent energy and transmission constraints. Global communities and organizations are facilitating and coordinating efforts to scale-up IoT technology, since this could lead to an enhanced, secured and efficient communication environment of connected living. Next generation networks will involve vertical markets such as automotive, energy, food and agriculture, city management, government, healthcare, manufacturing, public transportation, and so forth [2]. The demand for high speed and ultra reliable communications is growing rapidly, thus making the IoT a research hotspot.

One factor expected to play an important role in IoT infrastructure is 5G technology. Due to the promising increase in capacity, reduction in end-to-end latency, better reliability, and improvement in coverage, 5G holds the potential to address even the most demanding IoT requirements. More specifically, 5G IoT discloses enormous opportunities for connecting small size, low cost, typically battery-powered, and often densely populated devices to perform massive machine-type communications. Billion smart entities (e.g. sensors, actuators) are expected to be deployed worldwide, while traditional battery operated devices will become outdated. Therefore, in order to deal with their energy requirements, new solutions such as devices with extended battery lifetime and devices that are wirelessly powered will be evolved [3]. At the same time, all these IoT devices should target to small energy requirements in order to transmit their messages [4]. As such backscatter communication, is gaining popularity as a suitable solution to fulfill these needs. It is a mature technology that is successfully used in several applications e.g. smart homes and cities [5], biomedical field [6], environmental monitoring systems [7], vehicle monitoring [8] and sensor networks [9].

Backscatter communication systems can be clasified into three major types based on their architecture: monostatic, bistatic and ambient backscatter communication systems [10]. All the schemes share the same fundamentals. Particularly, a part of the received signal from the RF source, is backscattered to the reader node (RN), while the backscatter tag (BT) can send its data by tuning its antenna impedance to different states. This scheme is known as load modulation and in literature is largely confined to binary, due to hardware constraints. Though higher order modulator designs have been successfully prototyped [11], therefore more than a two-state modulation may be adopted [12]. The rest of the received signal from the RF source, is used by the BT for harvesting energy, thus making it possible to operate exclusively its own integrated circuit or partially support it, in terms of energy required.

On the other hand, by taking into consideration the architecture type, there are some differences. Specifically, in a bistatic communication system, the RF source and the receiver are separated, in contrast to the monostatic architecture where these two are integrated e.g. radio frequency identification

E. Goudeli, C. Psomas, and I. Krikidis are with the IRIDA Research Centre for Communication Technologies, Department of Electrical and Computer Engineering, University of Cyprus, Cyprus, e-mail:{egoude01, psomas, krikidis}@ucy.ac.cy.

This work was co-funded by the European Regional Development Fund and the Republic of Cyprus through the Research and Innovation Foundation, under the projects INFRASTRUCTURES/1216/0017 (IRIDA), POSTDOC/0916/0256 (IMPULSE) and EXCELLENCE/1216/0376 (SWITCH). It has also received funding from the European Research Council (ERC) under the European Union's Horizon 2020 research and innovation programme (Grant agreement No. 819819).

(RFID) reader. In the case of the monostatic architecture, as the RF source and the backscatter receiver are placed on the same device, the modulated signal may suffer from round-trip path loss [13], while near-far problem may be one of this architecture's limitations. In addition, in case where the backscatter transmitter is located far from the reader, due to signal loss from the RF source, it experiences higher energy outage probability and degradation of the received modulated backscatter signal strength [14]. Conversely, in the bistatic architecture, these problems may be mitigated [15], due to differentiated distance between the RF source, the BT and the RN. Finally, for the third type of ambient backscatter communication systems [16], the transmitter is separated from the backscatter receiver, but there is no dedicated RF source. Any available and opportunistic ambient source, like TV towers and cellular base stations, may be used as an RF source transmitter.

Regarding the detection method of the modulated signals from the BT to the RN, there are plenty of mechanisms proposed in the literature. The differences depend on the architecture applied, the modulation scheme adopted in the BT and the number of antennas used. More specifically, non-coherent detection is mainly adopted in ambient backscatter communications [17], where the knowledge of channel state information (CSI) at the RN is a challenging task. However, coherent detection may be adopted especially in the bistatic architecture, since the RF sources are most of the time devoted transmitters, that may set no restrictions to communication range and at the same time increase the bit rate [18]. As such, maximum-likelihood (ML) detectors can be applied at the RN so as to detect efficiently the received modulated signal [19].

Another characteristic that makes backscatter communications even more attractive for 5G IoT solutions, is the ability to enhance the BT with multiple antennas. The multiple antenna tag channel was first studied in [20], providing details for the behavior of the multiple-input multiple-output (MIMO) RFID channel. Later in [21], an orthogonal space-time coding scheme (OSTBC) was studied, proving that when employed and implemented in a MIMO RFID scenario, full diversity may be achieved. Numerous studies in literature prove the added value of multiple antennas in a backscatter communication system, providing enhanced performance in terms of spectral efficiency, bit rate and error probability [22]. At the same time, with the advances in printed antennas and RF micro-electronic technologies [23], multiple antennas can be integrated successfully into a device, while keeping the hardware cost low. It has to be noted, that the hardware request for a multiple antenna BT is currently a mature technology in terms of theoretical analysis and hardware implementation [24].

Furthermore, we herein consider multiple antenna techniques that have been proposed and studied in traditional MIMO systems, resulting in enhanced performance and increased spectral efficiency. More specifically, a generalized spatial modulation (GSM) technique, was presented in [25]. In GSM the transmitted information exploits the traditional modulation scheme and the antenna index as an additional source of information. Spatial modulation (SM) technique was first introduced by Mesleh *et al*. [26], [27] and is the simplified case of GSM, for one transmitting antenna at a time instant. The GSM scheme increases the overall spectral efficiency compared to SM, resulting in reduced number of transmit antennas for the same spectral efficiency. As an evolution to GSM, another spatial modulation-based technique, expanded in time domain, was introduced in [28]. In particular, Alamouti scheme [29] was applied in two out of the multiple transmitting antennas. Alamouti is a simple transmit diversity scheme, without any feedback from the receiver to the transmitter, with small computation complexity and no bandwidth expansion. Taking into consideration, that this coding scheme involves the transmission of multiple copies of the data, diversity gains are achievable for the given number of transmit and receive antennas.

Motivated by the above, in this work, we address two critical features of 5G IoT; wireless powered devices of low power consumption and high data rates. As such, we investigate a backscatter communication system with a multiple antenna BT. In contrast to the aforementioned works, we consider a bistatic architecture where spatial-modulation based techniques are employed at the BT and coherent detection is considered at the RN. To the best of our knowledge, this problem has not been addressed before in the literature. Recent attempts have been devoted in studying the advantages of spatial modulation-based techniques in backscatter communication systems, but in different context. More specifically, in [30], the authors study SM technique, over an ambient backscatter communication system with noncoherent detection. Furthermore, in [31], the GSM technique is applied at the source and not at the BT as we propose, while a cooperative detector based on the framework of sparse Bayesian learning is adopted, over an ambient backscatter architecture.

Our target is to exploit the advantages of a bistatic backscatter architecture with the use of sophisticated physical layer tools, provide a general mathematical framework and propose a system model that can be adopted from the majority of next generation IoT applications. Specifically, the main contributions of our study are as follows:

- With the use of multiple antennas at the BT, we apply sophisticated spatial modulation-based techniques. This enables us to increase the overall system efficiency, which is a key point for a 5G IoT solution. More specifically, with the use of GSM technique, we succeed enhanced performance in terms of SER, while at the same time reduce the number of transmit antennas needed in the BT. Furthermore, we examine the GSMA technique, where the transmitted information symbols are expanded to the time domain. With the use of Alamouti scheme, we succeed transmit diversity and ensure significant improvements in SER performance.
- We derive analytical expressions regarding the pairwise error probability for all the examined techniques, providing tight upper bounds. Furthermore, we asymptotically analyze the performance of our proposed system model, which yields insights to the limits' behavior, similar to [32], while at the same time proves the diversity order of GSM, SM and GSMA. Simulation results validate

the enhanced performance of the proposed techniques, emphasizing the strengths of each case.

The remaining part of this paper is organized as follows: in Section II we introduce the system model, whereas in Section III, spatial modulation-based techniques are examined in a multiple antenna BT along with their corresponding performance analysis. Numerical results that corroborate our analysis are presented in Section IV, while conclusions are drawn in Section V.

Notation: $||x||$ denotes the Euclidean norm of $x \in \mathbb{C}$, $\hat{x}$ denotes the estimation of variable x, while $Q(x) = \frac{1}{\sqrt{2\pi}} \int_x^\infty \exp(-\frac{u^2}{2})du$ denotes the Q-function and σ_x^2 denotes the variance of the variable x. Furthermore, $\Re\{x\}$ and $\Im\{x\}$ denote the real and imaginary parts of variable x, while with x^*, we denote the complex conjugate of x. We also use $\binom{n}{k}$, $\lfloor . \rfloor$ and $\lceil . \rceil$ for the binomial coefficient, the floor and the ceiling function of x, respectively. In addition, $\mathbf{x}$ is considered a $n \times 1$vector, while $\mathbf{X}$ denotes a $n \times m$ matrix, $\mathbb{E}[x]$ represents the expected value of x and $\lfloor x \rfloor_{2^p}$ is used in order to denote the largest integer less than or equal to x, that is an integer power of 2.

II. System Model & Backscatter Transmission Techniques

In this section, we provide all the details regarding the considered system model; the main mathematical notation related to the system model is summarized in Table I.

A. Topology and System Design

We study a bistatic backscatter communication system consisted of an RF source equipped with a single antenna, a BT with L antennas, out of which $L_u \in (1, L)$ are the active transmitting antennas at each time instant and a RN, also equipped with a single antenna. A schematic diagram of the considered backscatter network is shown in Fig. 1. Furthermore, we are assuming that the antennas at the RF source, the BT and the RN are spaced sufficiently far apart so that fading at each antenna is statistically independent. The RF source which is deployed for the backscatter system, broadcasts a continuous wave (CW) signal. The BT will then backscatter a portion of the received signal to the RN, by using appropriate load modulation. More specifically, the BT, actually transmits its own tag information when reflecting the signal, by switching its load impedance between different states. A portion of the CW signal is used by the BT to harvest energy and operate its own integrated circuit.

A complete chain of communication between the RF source and the RN, consists of two single paths: i) the forwarded unmodulated signal from the RF source to the multiple antennas BT and ii) the backscattered modulated signal from the multiple antenna BT to the RN. A model that captures these features is the dyadic backscatter channel (DBC) [20]. We herein assume that due to deep scattering and obstacles, the direct link between the RF source and the RN is not feasible [33], [34], [35]. Furthermore, in our study we mainly assume the sub-6 GHz band. We consider Rayleigh fading channel, due to its analytical and tractable results. Thus the forwarded and backscattered paths, are represented with independent and identically distributed (i.i.d.) complex Gaussian channel elements, while each element in DBC is drawn from $CN(0, 1)$.

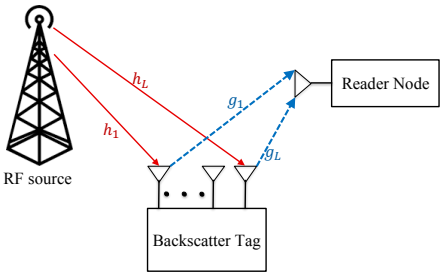

Fig. 1. Architecture of the bistatic backscatter network, consisting of an RF source, a multiple antenna BT and a RN equipped with one antenna.

It is worth noting, that all the channels are constant within a channel coherence time, though they may vary independently in different coherence intervals. In our study, we assume that for a specific time instant the load reflection coefficients for all the antennas in the BT, are the same. This results in a simultaneous transmission of a specific data symbol, from all the active transmitting antennas in the BT. Furthermore, for all the considered schemes studied, we assume that the detection at the RN is coherent and ML is adopted[1]. In addition, in our system model we apply element-based normalization, similar to [20] and [37]. Finally, the thermal noise at the BT could be negligible, since the tag includes only passive components related to the backscattering and involves little high intensity operation [19], [38].

B. Generalized Spatial Modulation (GSM)

In the case of GSM scheme, we examine one time slot, within L_u antennas are active and transmitting in the BT. The data symbol $x \in \mathbb{C}$, with $|\mathbb{C}| = M$, represents the symbol from the M-ary modulation scheme adopted in the BT, which is transmitted from all the L_u active antennas, at a time instant. Thus, the received signal at the RN is given by

$$r_{\text{GSM}} = \sqrt{P}\mathbf{F}_\ell \mathbf{x} + n, \tag{1}$$

where P is the average transmitted power from the RF source and n is the additive white Gaussian noise $\sim CN(0, \sigma_n^2)$, with $\sigma_n^2 = 1$, for the sake of simplicity. In addition, $\mathbf{x} \in \mathbb{C}^{L_u \times 1}$, is an $L_u \times 1$ vector with $x_i = x, \forall\ x_i \in (1, L_u)$. Finally, $\mathbf{F}_\ell$ is the DBC, regarding the schematic diagram of Fig. 1 and can be described using a row vector as follows

$$\mathbf{F}_\ell = \underbrace{\begin{bmatrix} h_{\ell_1} g_{\ell_1} & \cdots & h_{\ell_4} g_{\ell_4} & \cdots & h_{\ell_{L_u}} g_{\ell_{L_u}} \end{bmatrix}}_{L_u \text{ elements}}, \tag{2}$$

[1]To coherently detect the backscattered signal, we assume knowledge of the CSI at the RN, which is estimated on a short-term basis. Specifically, a known training signal is initially transmitted, therefore the CSI is estimated using the combined knowledge of the transmitted and the received signal at the RN, with the use of maximum likelihood or other estimation technique [36].

TABLE I
SUMMARY OF NOTATION

Notation	Description	Notation	Description
L	Total number of antennas in the BT	L_u	Number of active transmitting antennas in the BT $\in (1, L)$
P	Average transmitted power from the RF source	$\mathbf{F}_\ell$	DBC of the antenna set ℓ
x	M-ary data symbol in GSM & SM	x_1, x_2	M-ary data symbol transmitted in first and second time interval in GSMA
h_{ℓ_i}, g_{ℓ_i}	Forwarded and backscattered channels of the DBC	n	Additive white Gaussian noise
ℓ	Set of active and transmitting antennas in the BT	ℓ_i	Index of the i-th antenna in the antenna combination ℓ
m_μ	Spectral efficiency of $\mu \in$ {GSM, SM and GSMA}	θ	Rotation angle used in GSMA
P_s^μ	Probability of error for $\mu \in$ {GSM and GSMA}	q	Total number of of independent terms in DBC
d_μ	Diversity order for $\mu \in$ {GSM and GSMA}	$\Pr(x \to \hat{x})$	Pairwise error probability
v	Total number of codebooks in GSMA	α	Number of codewords in the $v-1$ codebooks

where $\ell = (\ell_1, \ell_2, \cdots, \ell_{L_u})$ indicates the antenna combination of the L_u active and transmitting antennas out of L antennas in the BT, and ℓ_i indicates the index of the i-th antenna in the antenna combination ℓ. Furthermore, h_{ℓ_i}, represents the forwarded channel of the DBC, from the transmit antenna of the RF source to the i-th antenna in the antenna combination ℓ. In addition, g_{ℓ_i} represents the backscattered channel, from the i-th antenna of the antenna combination ℓ to the RN. One main observation is that for a specific time instant, the total channel gain at the RN is simplified to $F_\ell = \sum_{i=1}^{L_u} h_{\ell_i} g_{\ell_i}$, while the data symbol transmitted, to a scalar $x \in \mathbb{C}$.

The spectral efficiency (bits/s/Hz) achieved with the GSM technique is

$$m_{\mathrm{GSM}} = m_c + \log_2 M, \tag{3}$$

where $m_c = \lfloor \log_2 \binom{L}{L_u} \rfloor$.

The optimal metric applied on the RN for the ML decision is given by

$$\left[\hat{x}, \hat{\ell}\right] = \arg\min_{\hat{x}, \hat{\ell}} \left\| r_{\mathrm{GSM}} - \sqrt{P} \sum_{i=1}^{L_u} \hat{h}_{\ell_i} \hat{g}_{\ell_i} \hat{x} \right\|^2, \tag{4}$$

where $\hat{h}_{\ell_i}$, $\hat{g}_{\ell_i}$ are the estimated forwarded and backscattered channels of DBC, respectively, from the estimated set of active transmitting antennas $\hat{\ell}$; and $\hat{x}$ is the estimated data symbol from the M-ary constellation scheme adopted in the BT.

SM is studied as a simplified scheme of GSM. From the L existing antennas in the BT, only one antenna remains active during transmission. Thus, the received signal at the RN and the optimal metric applied for the ML decision are given by (1) and (4), respectively, if we set $L_u = 1$. The spectral efficiency (bits/s/Hz) of the SM scheme is

$$m_{\mathrm{SM}} = \log_2(LM). \tag{5}$$

C. Generalized Spatial Modulation with Alamouti (GSMA)

In case of Alamouti OSTBC scheme, two antennas are active in two time slots. Furthermore, two data symbols x_1 and x_2 are transmitted in these two time slots, where $x_i \in \mathbb{C}$, with $i = 1, 2$ and $|\mathbb{C}| = M$. More specifically, these two data symbols are drawn from the M-ary constellation adopted and transmitted in an orthogonal manner, described by the codeword

$$\mathbf{X} = (\mathbf{x}_1 \ \mathbf{x}_2) = \begin{pmatrix} x_1 & x_2 \\ -x_2^* & x_1^* \end{pmatrix}, \tag{6}$$

where columns and rows correspond to the number of transmit antennas and the symbol interval, respectively. In our study we use Alamouti OSTBC in combination with GSM, as already described and introduced in [28], while the general system model follows the previous description. The codewords described in (6) are extended to the antenna domain and used in order to compose the codebooks. Each codebook is consisted of codewords, that should not have overlapping columns between them.

Furthermore, a rotation angle θ is considered, in order to ensure maximum diversity and coding gain at the expense of expansion of the signal constellation [28, Eq.(10)]. In case where θ is not considered, the resulting overlapping columns of codeword pairs from different codebooks reduces the transmit diversity order to one. In case of a bistatic backscatter communication system, with four antennas at the BT, the following four codewords are created

$$\begin{aligned} \chi_1 =& \left\{\mathbf{X}_{11}, \mathbf{X}_{12}\right\} \\ =& \left\{ \begin{pmatrix} x_1 & x_2 & 0 & 0 \\ -x_2^* & x_1^* & 0 & 0 \end{pmatrix}, \begin{pmatrix} 0 & 0 & x_1 & x_2 \\ 0 & 0 & -x_2^* & x_1^* \end{pmatrix} \right\}, \end{aligned} \tag{7}$$

and

$$\begin{aligned} \chi_2 =& \left\{\mathbf{X}_{21}, \mathbf{X}_{22}\right\} \\ =& \left\{ \begin{pmatrix} 0 & x_1 & x_2 & 0 \\ 0 & -x_2^* & x_1^* & 0 \end{pmatrix}, \begin{pmatrix} x_2 & 0 & 0 & x_1 \\ x_1^* & 0 & 0 & -x_2^* \end{pmatrix} \right\} \\ & \times \exp(j\theta). \end{aligned} \tag{8}$$

By taking into consideration the expand in time domain and specifically in two time intervals, the received signal in the RN is a 2×1 vector, which due to the orthogonality of the Alamouti's OSTBC, may be equivalently obtained by [28, Eq.(16)]

$$\mathbf{r}_{\mathrm{GSMA}} = \sqrt{P} \mathbf{F}_\ell \begin{bmatrix} x_1 \\ x_2 \end{bmatrix} + \mathbf{n}, \tag{9}$$

where $\mathbf{F}_\ell$ is a 2×2 equivalent channel matrix of the Alamouti coded GSM scheme, equal to

$$\mathbf{F}_\ell = \begin{bmatrix} h_{\ell_1} g_{\ell_1} \theta & h_{\ell_2} g_{\ell_2} \theta \\ (h_{\ell_2} g_{\ell_2} \theta)^* & -(h_{\ell_1} g_{\ell_1} \theta)^* \end{bmatrix}. \tag{10}$$

Similarly with GSM, h_{ℓ_1} and h_{ℓ_2}, represent the forwarded channels of the DBC to the first and second active transmitting antenna of set ℓ, in the BT. Likewise, g_{ℓ_1} and g_{ℓ_2} represent the backscattered channels, from the first and second active transmitting antenna of the set ℓ, to the RN. Furthermore, $\mathbf{n}$ is a 2×1 vector representing the AWGN $\sim CN(0, \sigma_n^2 \mathbf{I})$.

Thus the spectral efficiency (bits/s/Hz) for the GSMA scheme is

$$m_{\mathrm{GSMA}} = \frac{1}{2} \log_2 c + \log_2 M, \tag{11}$$

where c denotes the total number of codewords in GSMA and is given by

$$c = \lfloor \binom{L}{2} \rfloor_{2^p}, \tag{12}$$

where p is a positive integer.

During two consecutive symbols intervals, the bits transmitted from the BT are $2m_{\mathrm{GSMA}}$, where the first $\log_2 c$ bits determine the antenna pair combination, while the last $2\log_2 M$ bits determine the data symbol pair (x_1, x_2). Taking into consideration the spectral efficiency of Alamouti's OSTBC, which is given by $m_{\mathrm{Alamouti}} = \log_2 M$ bits/s/Hz, we observe an increment of $\frac{1}{2}\log_2 c$ bits/s/Hz for GSMA.

Regarding the ℓ-th set of active transmitting antennas combination in the BT, the receiver in the RN uses the decomposition as followed in [39] and determines the associated minimum ML metrics $e_{1,\ell}$ and $e_{2,l}$ for x_1 and x_2, resulting from the orthogonality of $\mathbf{f}_{\ell_1}$ and $\mathbf{f}_{\ell_2}$, as

$$e_{1,\ell} = \arg\min_{x_1 \in \mathbb{C}} \left\| \mathbf{r}_{\mathrm{GSMA}} - \sqrt{P}\mathbf{f}_{\ell_1} x_1 \right\|^2, \tag{13}$$

$$e_{2,\ell} = \arg\min_{x_2 \in \mathbb{C}} \left\| \mathbf{r}_{\mathrm{GSMA}} - \sqrt{P}\mathbf{f}_{\ell_2} x_2 \right\|^2, \tag{14}$$

where $\mathbf{F}_\ell = [\mathbf{f}_{\ell_1}, \mathbf{f}_{\ell_2}]$. Since $e_{1,\ell}$ and $e_{2,\ell}$ are calculated by the ML decoder for the ℓ-th set of active transmitting antennas, their summation $e_\ell = e_{1,\ell} + e_{2,\ell}$ gives the total ML metric for the ℓ-th set. Finally, the receiver at the RN makes a decision by choosing the minimum antenna combination metric as $\hat{\ell} = \arg\min_{\ell} e_\ell$.

III. Performance Analysis

In this section, we analytically derive the PEP for the studied techniques (GSM, SM and GSMA) applied in our bistatic backsatter system model, investigating the union bound for the probability of error, in each case. Finally, in the last part we further investigate the enhanced performance succeeded from GSMA, by analyzing the diversity order.

A. Pairwise Error Probability for GSM and SM

We further proceed by following the steps proposed in [25], in order to calculate the PEP for GSM technique. More specifically, the GSM modulated signal is backscattered from the L_u active antennas of the BT over the DBC channel. By taking into consideration the euclidean distances, the pairwise probability of error is computed

$$\Pr(x_\ell \to \hat{x}_{\hat{\ell}}) = \Pr\left(\|D(\ell, x)\|^2 > \|D(\hat{\ell}, \hat{x})\|^2 \right), \tag{15}$$

where x_ℓ indicates the data symbol $x \in M$-ary modulation, that is transmitted from a set of antennas combination ℓ. In addition, $\hat{x}_{\hat{l}}$ indicates the estimated M-ary data symbol $\hat{x}$, which is transmitted from an estimated set of antennas combination $\hat{\ell}$. Furthermore, $\Pr(x_\ell \to \hat{x}_{\hat{\ell}})$ denotes the PEP on deciding $\hat{x}_{\hat{\ell}}$, while x_ℓ is actually transmitted. PEP highly depends on the squared Euclidean distance between the pairs of the transmitted and estimated spatial symbols, denoted as $\|D(\ell, x)\|^2$ and $\|D(\hat{\ell}, \hat{x})\|^2$, respectively. Recalling the expression in (1), we further proceed with

$$D(\ell, x) = r_{\mathrm{GSM}} - \sqrt{P}F_\ell x = n. \tag{16}$$

Taking into consideration that $\hat{F}_\ell = \sum_{i=1}^{L_u} \hat{h}_{\ell_i}\hat{g}_{\ell_i}$, we can express $D(\hat{\ell}, \hat{x})$ as

$$\begin{aligned} D(\hat{\ell}, \hat{x}) &= r_{GSM} - \sqrt{P}\hat{F}_\ell \hat{x} \\ &= n + \sqrt{P}\left(\sum_{i=1}^{L_u} h_{\ell_i} g_{\ell_i} x - \sum_{i=1}^{L_u} \hat{h}_{\ell_i}\hat{g}_{\ell_i}\hat{x} \right). \end{aligned} \tag{17}$$

With the proper substitutions and calculations, we state the following Proposition.

Proposition 1. *The PEP for GSM is upper bounded by*

$$Pr(x_\ell \to \hat{x}_{\hat{\ell}}|q) \le \int_0^\infty Q\left(\sqrt{\gamma_n}\right) f_{\gamma_n}(\gamma_n) d\gamma_n, \tag{18}$$

where q is a non-negative integer and denotes the number of independent terms that consist the DBC, γ_n, for each pair of estimated symbols $(x_\ell, \hat{x}_{\hat{\ell}})$. In addition $f_{\gamma_n}(\gamma_n)$ is the probability density function (pdf) of γ_n and is given as [21, Eq.(8)]

$$f_{\gamma_n}(\gamma_n) = \frac{2\gamma_n^{(q-1)/2}}{(q-1)!\hat{\gamma}^{(q+1)/2}} K_{q-1}\left(2\sqrt{\frac{\gamma_n}{\hat{\gamma}}}\right), \tag{19}$$

where $K_{q-1}(\cdot)$ denotes the modified Bessel function of the second kind and $\hat{\gamma} = P/2$ is the average power at the RN.

Proof. See Appendix A. □

Note that the q is numerically evaluated. Specifically the set of values is $\{0, 1, 2, \ldots, N_3\}$, where $N_3 = L_u x_R + L_u x_I + L_u \hat{x}_R + L_u \hat{x}_I$, with $x_R \approx \Re\{x\}$, $x_I \approx \Im\{x\}$, $\hat{x}_R \approx \Re\{\hat{x}\}$ and $\hat{x}_I \approx \Im\{\hat{x}\}$. One main observation regarding the possible values of q is that when the decoding is successful, i.e $\hat{x}_{\hat{\ell}} = x_\ell$, then $q = 0$, while when neither the antennas nor the data symbol are correctly estimated, then $q = N_3$.

We herein calculate the probability of error in terms of SER for GSM, by defining an upper bound for the union of the events. The events taken into consideration and summed up for the calculation of the union bound, are all the PEP for all the possible combinations, in terms of the estimated active transmitting antennas and the estimated data symbol from the M-ary modulation scheme. Thus, the union bound for the probability of error in terms of SER, regarding the GSM scheme, is given by

$$\mathrm{P}_s^{\mathrm{GSM}} \le \sum_{i=2}^{N_1} \Pr(x_1 \to \hat{x}_i|q), \tag{20}$$

where $N_1 = M\binom{L}{L_u} - 1$ and $\Pr(x_i \to \hat{x}_i|q)$ is given by (18). The PEP and SER for the simplified case of SM technique, follow the same analysis as in GSM, by considering only one transmitting antenna, i.e. $L_u = 1$.

B. Pairwise Error Probability for GSMA

In the following, before proceeding to the calculation of PEP, we summarize the steps needed to be followed in order to design the GSMA, considering the proper codewords, codebooks and rotation angles.

1) Given the total number of transmit antennas in the BT, L, we calculate the number of possible antenna combinations for the transmission of Alamouti's OSTBC. The number of possible antenna combinations is $\binom{L}{L_u}$. However, the number of antenna combinations that can be considered for transmission must be a power of two. Therefore, only $L_c = 2^{m_c}$ combinations, can be used, where $m_c = \lfloor \log_2 \binom{L}{L_u} \rfloor$.
2) We proceed by calculating the total number of codewords c, given by (12).
3) We calculate the number of codewords in each codebook $\chi_i, i = 1, 2, \cdots, v-1$ from $\alpha = \lfloor L/2 \rfloor$ and the total number of codebooks from $v = \lceil c/\alpha \rceil$. Note, that the last codebook χ_v does not need to have α codewords, i.e. its cardinality is $\alpha' = c - \alpha(v-1)$.
4) We construct the codebooks, considering the following two facts, i.e.:
   a) each codebook must contain non-interfering codewords chosen form the pairwise combinations of L transmitting antennas in the BT,
   b) each codebook must be composed of codewords with antenna combinations that were never used in the construction of a previous codebook.
5) We use the appropriate rotation angle θ_i, for each codebook χ_i, based on the signal constellation and the antenna configuration, as optimally calculated per case in [28, Eq.(10)]. More specifically

$$\theta_i = \begin{cases} \frac{(i-1)\pi}{v}, & \text{for BPSK} \\ \frac{(i-1)\pi}{2v}, & \text{for QPSK.} \end{cases} \tag{21}$$

The performance analysis of the proposed GSMA scheme, is now focused on calculating $\Pr(\mathbf{X} \to \hat{\mathbf{X}})$, which is the PEP of deciding matrix $\hat{\mathbf{X}}$ when $\mathbf{X}$ is transmitted. Following the proper analysis, the next Proposition is formed.

Proposition 2. *The PEP of GSMA is upper bounded by*

$$Pr(\boldsymbol{X} \to \hat{\boldsymbol{X}}|q) \leq \int_0^\infty \int_0^\infty Q\left(\sqrt{\gamma_1 + \gamma_2}\right) f_{\gamma_1}(\gamma_1)\, d\gamma_1 \times f_{\gamma_2}(\gamma_2)\, d\gamma_2, \tag{22}$$

where f_{γ_i} denotes the pdf of the transmitted DBC at time instant $i \in (1, 2)$ and is given by (19).

Proof. See Appendix B. □

Having identified the PEP for GSMA from (22) and taking into consideration the pdf from (19), we may proceed to calculate the union bound for the probability of error, in terms of SER. It has to be noticed that due to the symmetry of the codebooks, all the transmission matrices have the uniform error property, i.e. have the same PEP as that of $\mathbf{X}_{11}$ [28, Eq.(24)]. Thus, we obtain the upper bound as follows

$$\mathrm{P}_s^{\mathrm{GSMA}} \leq \sum_{j=2}^{\alpha} \Pr(\mathbf{X}_{11} \to \mathbf{X}_{1j}|q) + \sum_{i=2}^{v-1} \sum_{j=1}^{\alpha} \Pr(\mathbf{X}_{11} \to \mathbf{X}_{ij}|q) + \sum_{j=1}^{\alpha'} \Pr(\mathbf{X}_{11} \to \mathbf{X}_{vj}|q), \tag{23}$$

where we recall here that v is the total number of codebooks, α is the total number of codewords in the $v-1$ codebooks, α' is the number of codewords in the last codebook v and $\Pr(\mathbf{X}_{11} \to \mathbf{X}_{ij})$ is given by (22).

C. Diversity Analysis

In this section we investigate the diversity order of our system model for the spatial modulation-based communication techniques studied. The diversity order d of the system is the asymptotic rate at which the probability of error P_s decays, as a function of average transmitted power P and is defined as

$$d_\mu = \lim_{P \to \infty} -\frac{\log \mathrm{P}_s^\mu}{\log P}, \tag{24}$$

where $\mu \in \{\text{GSM and GSMA}\}$. Taking into consideration the expression for the SER given by (20) and by (23), regarding the GSM and GSMA technique, respectively, the next Proposition is formed.

Proposition 3. *The diversity order regarding the GSM and SM technique is equal to one, i.e. $d_{\mathrm{GSM}} = 1$, while for GSMA technique is equal to two, i.e. $d_{\mathrm{GSMA}} = 2$.*

Proof. See Appendix C. □

A key conclusion from the above is that by applying a combination of the Alamouti scheme and the spatial techniques in a multiple antenna BT, there is an enhanced and improved probability of error for the detection of transmitted symbols and transmitting antennas in the RN. More specifically, we can conclude that increasing the number of transmit/receive antennas in the BT, while applying the spatial techniques of GSM and SM, one can succeed array gain. Further expanding, with the use of GSMA, we exploit also the time domain and manage to succeed transmit diversity $d_{\mathrm{GSMA}} = 2$.

IV. Numerical Results

In this section, we provide numerical results in order to verify the enhanced performance achieved by our proposed spatial modulation-based techniques, GSM, SM and GSMA, when applied to the considered system model. We evaluate their performance in terms of SER, targeting the same spectral efficiency and we further study and present their behavior in terms of spectral efficiency, while varying the number of antennas in the BT. More specifically, computer simulations are carried out and all the outcomes presented are calculated with the use of 10^5 iterations.

In Fig. 2 and Fig. 3, all the three schemes studied, are presented comparatively in terms of SER. With the continuous line, we present the performance of a single input single output

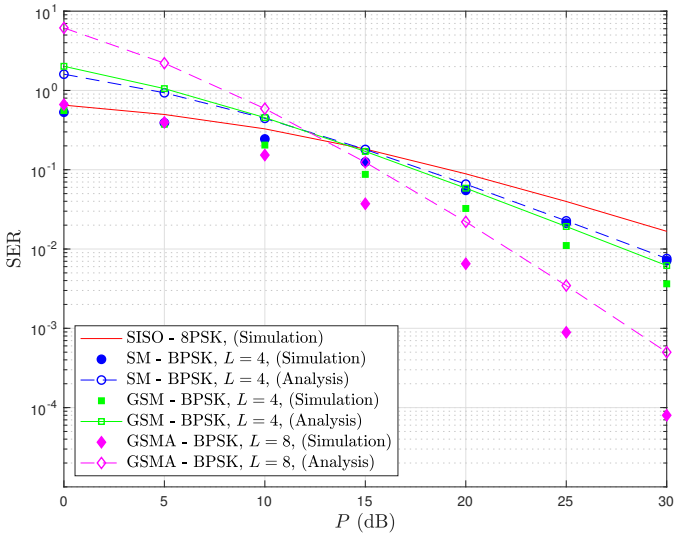

Fig. 2. Comparison of GSM, SM and GSMA with a spectral efficiency 3 bits/s/Hz.

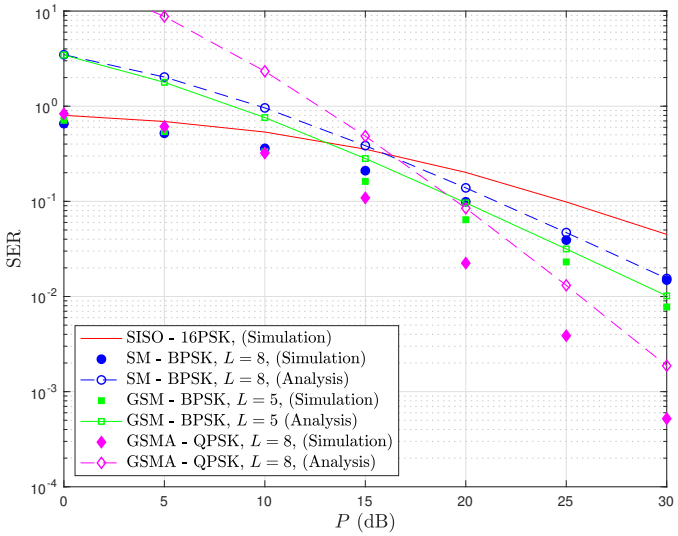

Fig. 3. Comparison of GSM, SM and GSMA with a spectral efficiency 4 bits/s/Hz.

(SISO) bistatic backscatter system with only one antenna in the BT, i.e. $L = 1$, as a metric of comparison to our proposed spatial modulation-based techniques. As expected, such a solution constitutes an upper bound for GSMA, GSM and SM. On the other hand, GSMA with the use of combined spatial and time modulation, manages to overcome the other two techniques, in terms of SER. In addition, GSM and SM, although they improve the performance of the studied backscatter system, they manage to achieve similar results in terms of SER.

The targeted spectral efficiency, regarding the evaluated simulation results presented in Fig. 2 and Fig. 3, is 3 bits/s/Hz and 4 bits/s/Hz, respectively. In order to succeed this, we combined $L = 4, 5, 8$ transmitting antennas with several modulation schemes in the BT, i.e. 16PSK, 8PSK, BPSK and QPSK. Another observation from Fig. 2 and Fig. 3, is that the derived union bounds, consist tight upper bounds compared

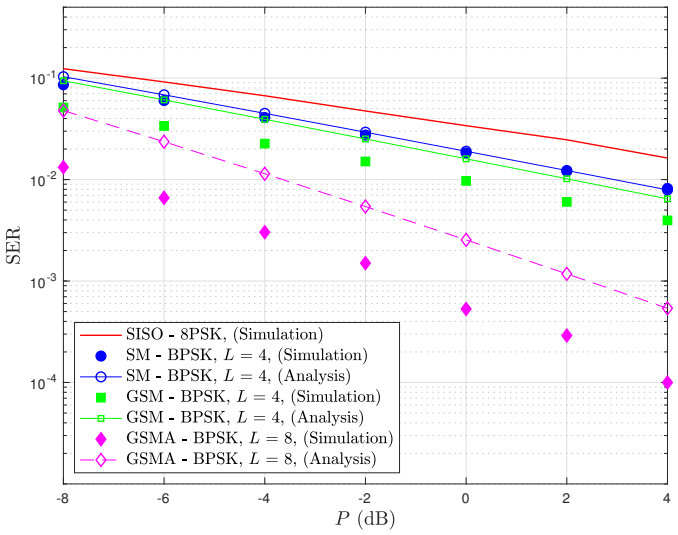

Fig. 4. Comparison of GSM, SM and GSMA with a spectral efficiency 3 bits/s/Hz and practical numerical setup.

to the simulations of all the three spatial modulation-based techniques. More specifically, the union bound that is adopted in our paper, is quite sharp and is traditionally used in the literature as an appropriate upper bound for the pairwise error probabilities [40]. It is noteworthy that when increasing the number of antennas in the BT, there are more combinations to estimate at the RN, consequently more pairwise error probability terms appear and the gap between the upper bound and the simulation increases. Same behavior is noticed, when we extend our study in two time slots with the use of GSMA technique. On the other hand, when we increase the transmit power we notice that this gap smooths, which is an expected trade off. Finally, with the increase of the targeted spectral efficiency, the performance in terms of SER for all the spatial schemes studied, is slightly deteriorated.

In Fig. 4 we apply the mathematical framework for a practical setting, based on an indoor application [5]. More specifically, the RF source communicates with BT with a bandwidth of 2 MHz. The path loss effect is taken into consideration, while the distances between the RF source, the BT and the RN are 5 m and 6 m, respectively. It has to be noticed, that the behavior of our system model follows the same trends, as in Fig. 2 and Fig. 3. More specifically, GSMA technique prevails over GSM and SM, succeeding transmit diversity and enhanced performance in terms of SER.

In Fig. 5, we present how the spectral efficiency of the considered schemes is affected, when varying the number of antennas in the BT. More specifically, the modulation scheme studied is kept common in all three cases, as BPSK. In addition, for the GSM and GSMA technique, the number of transmitting antennas each time instant is $L_u = 2$, out of totally L antennas in the BT. Recalling the spectral efficiencies of each technique, as described in Section II from (3), (5), and (11), some main observations are derived, that are also confirmed from the relative figure. Firstly, we clearly identify that for $L > 4$, the first term of GSM spectral efficiency is always greater than the other two schemes. As such, in order to

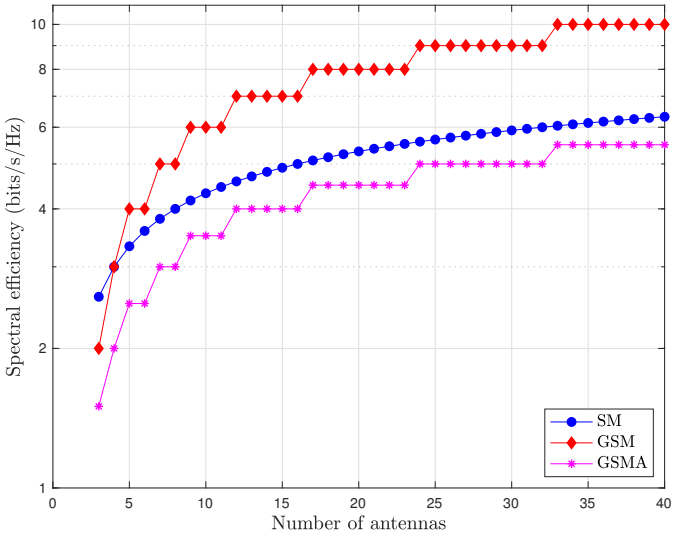

Fig. 5. Spectral efficiency comparison for GSM, SM and GSMA.

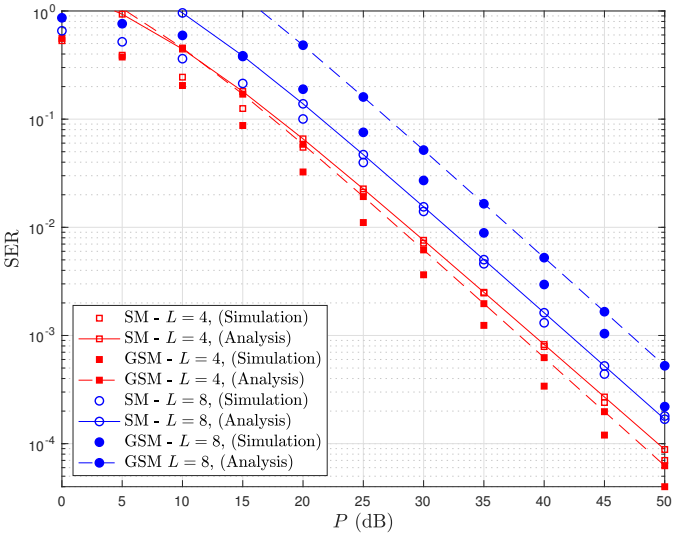

Fig. 6. Comparison of GSM and SM, for the same number $L = 4, 8$ of antennas.

transmit the same number of bits, there is needed a sufficient larger amount of antennas in the BT regarding SM and GSMA techniques. For example, in order to transmit 4 bits/s/Hz, the antennas needed in the BT are $L = 5$ or 6 for GSM, $L = 8$ for SM and $L = 12, \ldots, 16$ for GSMA. In addition, due to the floor operation in (3) and (11), the spectral efficiency for GSM and GSMA respectively, remains the same for a range of transmitting antennas.

Figs. 6 and 7, illustrate the performance of the two backscatter spatial MIMO techniques, specifically referring to GSM and SM. BPSK modulation is applied and the number of antennas at the BT is $L = 4, 8, 16, 32$. Regarding the GSM technique, we assume two active transmitting antennas i.e. $L_u = 2$. As expected, for the same number of antennas the SM scheme provides us with an enhanced performance in terms of SER. This is justified from the fact that the spectral efficiency for GSM is higher, resulting in a higher number of transmitted bits/s/Hz, thus increasing the probability of error when decoding. Furthermore, the comparatively enhanced performance of SM to GSM, is also justified due to the highest probability of error when detecting two active and transmitting antennas instead of only one.

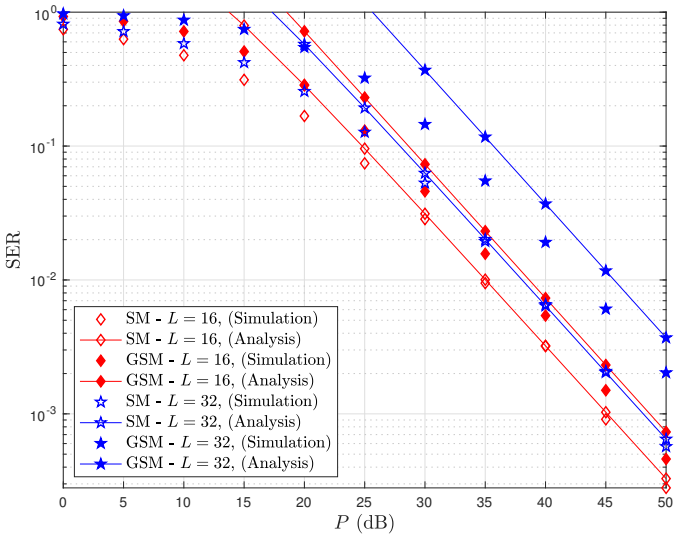

Fig. 7. Comparison of GSM and SM, for the same number $L = 16, 32$ of antennas.

V. Conclusion

In this paper, we propose the use of backscatter communication as a novel and high efficient solution for 5G IoT technology. The need of an IoT network is growing rapidly, targeting an interconnection of numerous small size, low cost and wireless self-powered devices. Backscatter communication seems to ideally serve the demands of such a network, since BTs are capable of transmitting their data, while at the same time may operate exclusively their own integrated circuit or partially support it, in terms of energy required, due to their harvesting capabilities. The ability of multiple antennas at the BT, gives us the opportunity to apply sophisticated spatial modulation-based techniques and achieve enhanced performance in terms of SER and spectral efficiency. Initially, we study the GSM technique, where we exploit the antenna index as an extra dimension for additional source of information. SM is also presented in our study as a special and simplified case of GSM, with only one transmitting antenna at a time instant. We further enhance our study in time domain, by proposing GSMA technique; with the use of Alamouti scheme in two transmitting antennas, we manage to improve significantly SER performance and succeed transmit diversity. Simulation and theoretical results are consistent, corroborating our proposal as an enhanced solution, in terms of overall efficiency. An interesting direction for future work is to re-evaluate the performance of our system model with non coherent detection schemes, as well as to extend our study into the millimeter wave frequency band.

APPENDIX A
PROOF OF PROPOSITION 1

Substituting (16) and (17) into (15), and assuming for a given DBC

$$\begin{aligned}
&\Pr(x_\ell \to \hat{x}_{\hat{\ell}}|F_\ell) \\
&= \Pr\left(\|n\|^2 > \left\| n + \sqrt{P}\left(\sum_{i=1}^{L_u} h_{\ell_i} g_{\ell_i} x - \sum_{i=1}^{L_u} \hat{h}_{\ell_i} \hat{g}_{\ell_i} \hat{x} \right) \right\|^2 \right) \\
&= \Pr\left(\frac{\sqrt{P}}{2} \left| \sum_{i=1}^{L_u} h_{\ell_i} g_{\ell_i} x - \sum_{i=1}^{L_u} \hat{h}_{\ell_i} \hat{g}_{\ell_i} \hat{x} \right|^2 < B \right), \qquad (25)
\end{aligned}$$

where

$$\begin{aligned}
B = &- \Re\left\{ n \left(\sum_{i=1}^{L_u} h_{\ell_i} g_{\ell_i} x - \sum_{i=1}^{L_u} \hat{h}_{\ell_i} \hat{g}_{\ell_i} \hat{x} \right) \right\} \\
&- \Im\left\{ n \left(\sum_{i=1}^{L_u} h_{\ell_i} g_{\ell_i} x - \sum_{i=1}^{L_u} \hat{h}_{\ell_i} \hat{g}_{\ell_i} \hat{x} \right) \right\}, \qquad (26)
\end{aligned}$$

so

$$\begin{aligned}
\sigma_B^2 = &\Re\left\{ \sigma_n^2 \left(\left| \sum_{i=1}^{L_u} h_{\ell_i} g_{\ell_i} x - \sum_{i=1}^{L_u} \hat{h}_{\ell_i} \hat{g}_{\ell_i} \hat{x} \right|^2 \right) \right\} \\
&+ \Im\left\{ \sigma_n^2 \left(\left| \sum_{i=1}^{L_u} h_{\ell_i} g_{\ell_i} x - \sum_{i=1}^{L_u} \hat{h}_{\ell_i} \hat{g}_{\ell_i} \hat{x} \right|^2 \right) \right\}, \qquad (27)
\end{aligned}$$

where $\Re\{n\}$ and $\Im\{n\}$, represent the real and imaginary parts of the additive white Gaussian noise n, respectively with $\Re\{n\}, \Im\{n\} \sim N(0, \frac{1}{2})$. Thus (25) becomes

$$\begin{aligned}
&\Pr(x_\ell \to \hat{x}_{\hat{\ell}}|F_\ell) \\
&= Q\left(\frac{\sqrt{P} \| \sum_{i=1}^{L_u} h_{\ell_i} g_{\ell_i} x - \sum_{i=1}^{L_u} \hat{h}_{\ell_i} \hat{g}_{\ell_i} \hat{x} \|^2}{2\sqrt{\frac{1}{2} \| \sum_{i=1}^{L_u} h_{\ell_i} g_{\ell_i} x - \sum_{i=1}^{L_u} \hat{h}_{\ell_i} \hat{g}_{\ell_i} \hat{x} \|^2}} \right) \\
&= Q\left(\sqrt{\frac{P \| \sum_{i=1}^{L_u} h_{\ell_i} g_{\ell_i} x - \sum_{i=1}^{L_u} \hat{h}_{\ell_i} \hat{g}_{\ell_i} \hat{x} \|^2}{2}} \right) \\
&= Q\left(\sqrt{\hat{\gamma} \left\| \sum_{i=1}^{L_u} h_{\ell_i} g_{\ell_i} x - \sum_{i=1}^{L_u} \hat{h}_{\ell_i} \hat{g}_{\ell_i} \hat{x} \right\|^2} \right) = Q\left(\sqrt{\gamma_n} \right), \qquad (28)
\end{aligned}$$

where $\hat{\gamma} = \frac{P}{2}$. In order to further proceed with the derivation of (18), we calculate the expected value of (28), by integrating it for all the possible values of F_ℓ, resulting in

$$\begin{aligned}
\Pr(x_\ell \to \hat{x}_{\hat{\ell}}|q) &= \mathbb{E}[\Pr(x_\ell \to \hat{x}_{\hat{\ell}}|F_\ell)] \\
&\leq \int_0^\infty Q\left(\sqrt{\gamma_n} \right) f(\gamma_n) d\gamma_n, \qquad (29)
\end{aligned}$$

where $f(\gamma_n)$ is the pdf of γ_n given by (19), as a function of q, which is a non-negative integer. The inequality in (29) results from the following assumption. Depending on the estimated pair symbol $(x_\ell \to \hat{x}_{\hat{\ell}})$, γ_n may result as a sum of either correlated or independent channels. For mathematical tractability and specifically for the case of the correlated channels, we consider an upper bound with good results as proved in [20], assuming that all the terms consisting of γ_n are independent. Taking into consideration that $x \in \mathbb{C}$, the real and imaginary parts of the terms consisting the norm of γ_n are rounded to the nearest integer. In addition, it has to be noted that due to the scaling property of a normal distribution, imaginary terms of γ_q, i.e. $-jh_{\ell_i} g_{\ell_i}$, may be treated as $h_{\ell_i} g_{\ell_i}$, while negative terms i.e. $-h_{\ell_i} g_{\ell_i}$ may be treated as $h_{\ell_i} g_{\ell_i}$.

Hence the expression of Proposition 1 is derived.

APPENDIX B
PROOF OF PROPOSITION 2

In our study of GSMA technique, the number of active antennas is $L_u = 2$ and we apply Alamouti OSTBC. The PEP for a given $\mathbf{F}_\ell$, is given with the use of [28, Eq.(21)] as

$$\Pr(\mathbf{X} \to \hat{\mathbf{X}}|\mathbf{F}_\ell) = Q\left(\sqrt{\frac{P}{2} \left\| \mathbf{F}_\ell (\mathbf{X} - \hat{\mathbf{X}}) \right\|^2} \right). \qquad (30)$$

Following the analysis in [41, Ch.7], we define a new matrix $\mathbf{A} = (\mathbf{X} - \hat{\mathbf{X}})(\mathbf{X} - \hat{\mathbf{X}})^H$. Because $\mathbf{A}$ is Hermitian, we can apply an eigenvalue decomposition and rewrite it, as $\mathbf{A} = \mathbf{U}\Lambda\mathbf{U}^H$, where $\mathbf{U}$ is a unitary matrix and Λ is a diagonal matrix with diagonal elements equal to the eigenvalues of the matrix $\mathbf{A}$. With the proper substitutions and calculations, we have

$$\left\| \mathbf{F}_\ell (\mathbf{X} - \hat{\mathbf{X}}) \right\|^2 = \mathbf{F}_\ell \mathbf{U} \Lambda \mathbf{U}^H \mathbf{F}_\ell^H = \sum_{i=1}^{L_u} \lambda_i \left\| \beta_i \right\|^2, \qquad (31)$$

where λ_i's are the eigenvalues of the matrix $\mathbf{A}$, calculated from $\|\mathbf{A} - \lambda\mathbf{I}\|^2 = 0$. In addition, β_i are the beta terms, which are functions of the DBC matrix and from (a) in (37), are given as $\beta_i = \sum_{j=1}^{L_u} u_{ji} h_{\ell_j} g_{\ell_j}$, with $i \in (1, L_u)$. Without loss of generality, we assume that the codewords are chosen as

$$\mathbf{X} = \begin{pmatrix} \mathbf{x}_1 & \mathbf{x}_2 & \mathbf{0}_{2\times(L-2)} \end{pmatrix}, \qquad (32)$$

and

$$\hat{\mathbf{X}} = \begin{pmatrix} \hat{\mathbf{x}}_1 & \mathbf{0} & \hat{\mathbf{x}}_2 & \mathbf{0}_{2\times(L-3)} \end{pmatrix} \exp(j\theta), \qquad (33)$$

where $j = \sqrt{-1}$ is the imaginary number and with $\mathbf{0}_{i\times j}$ we denote a small zero of i lines and j columns.

Then the matrix $\mathbf{A}$ is given as

$$\begin{aligned}
\mathbf{A} = &\begin{pmatrix} x_1 - \hat{x}_1 \exp(j\theta) & x_2 & -\hat{x_2} \exp(j\theta) & \mathbf{0}_{1\times(L-3)} \\ -x_2^* + \hat{x_2}^* \exp(j\theta) & x_1^* & -\hat{x_1}^* \exp(j\theta) & \mathbf{0}_{1\times(L-3)} \end{pmatrix} \\
\times &\begin{pmatrix} x_1^* - \hat{x}_1^* \exp(-j\theta) & -x_2 + \hat{x}_2 \exp(-j\theta) \\ x_2^* & x_1 \\ -\hat{x}_2^* \exp(-j\theta) & -\hat{x}_1 \exp(-j\theta) \\ \mathbf{0}_{(L-3)\times 1} & \mathbf{0}_{(L-3)\times 1} \end{pmatrix} \qquad (34) \\
= &\begin{pmatrix} k - \frac{x_1 \hat{x}_1^*}{\exp(j\theta)} - x_1^* \hat{x}_1 \exp(j\theta) & \frac{x_1 \hat{x}_2}{\exp(j\theta)} + x_2 \hat{x}_1 \exp(j\theta) \\ \frac{\hat{x}_1^* x_2^*}{\exp(j\theta)} + x_1^* \hat{x}_2^* \exp(j\theta) & k - \frac{x_2^* \hat{x}_2}{\exp(j\theta)} - x_2 \hat{x}_2^* \exp(j\theta) \end{pmatrix}, \qquad (35)
\end{aligned}$$

where $k = \sum_{i=1}^{2} \left(\|x_i\|^2 + \|\hat{x}_i\|^2 \right)$. Calculating, the eigenvalues λ_1 and λ_2, based on the estimated $\hat{x}_1, \hat{x}_2$ and the angle θ, we can proceed by solving the following system

$$\mathbf{A} \begin{bmatrix} u_{11} \\ u_{21} \end{bmatrix} = \lambda_1 \begin{bmatrix} u_{11} \\ u_{21} \end{bmatrix},$$

$$\mathbf{A}\begin{bmatrix} u_{12} \\ u_{22} \end{bmatrix} = \lambda_2 \begin{bmatrix} u_{12} \\ u_{22} \end{bmatrix}, \tag{36}$$

which results in calculating the elements $u_{ji} \in \mathbb{C}$ of the unitary matrix $\mathbf{U}$. With the use of existing numerical tools such as $eig(\cdot)$ function in Matlab [42], we can calculate reliably and efficiently the eigenvalues λ_i's of the matrix $\mathbf{A}$ and the u_{ji} terms of the unitary matrix $\mathbf{U}$. Therefore, (30) becomes

$$\begin{aligned}
&\Pr(\mathbf{X} \to \hat{\mathbf{X}} \mid \mathbf{F}_\ell) \\
&\overset{(a)}{=} Q\left(\sqrt{\frac{P}{2}\sum_{i=1}^{L_u}\lambda_i\left\|\sum_{j=1}^{L_u}u_{ji}h_{\ell_j}g_{\ell_j}\right\|^2}\right) \\
&= Q\Bigg(\sqrt{\frac{P}{2}\Big(\lambda_1\|u_{11}h_{\ell_1}g_{\ell_1}+u_{21}h_{\ell_2}g_{\ell_2}\|^2 \\
&\qquad + \lambda_2\|u_{12}h_{\ell_1}g_{\ell_1}+u_{22}h_{\ell_2}g_{\ell_2}\|^2\Big)^{\frac{1}{2}}}\Bigg) \\
&= Q\Bigg(\sqrt{\frac{P}{2}\Big(\lambda_1\|u_{11}\|^2\|h_{\ell_1}g_{\ell_1}+a_3h_{\ell_2}g_{\ell_2}\|^2 \\
&\qquad + \lambda_2\|u_{22}\|^2\|a_4h_{\ell_1}g_{\ell_1}+h_{\ell_2}g_{\ell_2}\|^2\Big)^{\frac{1}{2}}}\Bigg) \\
&= Q(\sqrt{\gamma_1+\gamma_2}),
\end{aligned} \tag{37}$$

where $a_3 = \frac{u_{21}}{u_{11}}$, $a_4 = \frac{u_{12}}{u_{22}}$, $\hat{\gamma_1} = \frac{P}{2}\lambda_1\|u_{11}\|^2$ and $\hat{\gamma_2} = \frac{P}{2}\lambda_2\|u_{22}\|^2$.

In order to proceed further with the derivation of PEP in GSMA, given by (22), we calculate the expected value of (37), for all possible values of $\mathbf{F}_\ell$, as follows

$$\begin{aligned}
\Pr(\mathbf{X} \to \hat{\mathbf{X}}|q) &= \mathbb{E}[\Pr(\mathbf{X} \to \hat{\mathbf{X}} \mid \mathbf{F}_\ell)] \\
&\leq \int_0^\infty\int_0^\infty Q(\sqrt{\gamma_1+\gamma_2})f_{\gamma_1}(\gamma_1)f_{\gamma_2}(\gamma_2)d\gamma_1 d\gamma_2,
\end{aligned} \tag{38}$$

where with $f_{\gamma_1}(\gamma_1)$ and $f_{\gamma_2}(\gamma_2)$, we denote the pdf of the DBC in the first and the second time instant respectively, while applying the Alamouti code, given by (19). The inequality in (38) results from the assumption taken into consideration in Proposition 1, i.e. for mathematical tractability, all the terms of the DBC consisting of γ_1 and γ_2 are considered as independent.

Hence the expression of Proposition 2 is derived.

Appendix C
Proof of Proposition 3

Taking into consideration the following improved exponential approximation for the Q-function [43]

$$Q(x) \approx \frac{1}{12}\exp\left(-\frac{x^2}{2}\right) + \frac{1}{4}\exp\left(-\frac{2}{3}x^2\right),\ x > 0 \tag{39}$$

as well as the approximations of the Bessel function [44], we obtain the following approximation regarding the pdf from (19), for high SNR i.e. $P \to \infty$, as

$$f_{\gamma_n}(\gamma_n) = \begin{cases} -\frac{1}{\hat{\gamma}}\ln\left(\frac{\gamma_n}{\hat{\gamma}}\right), & \text{if } q = 1, \\ \frac{1}{(q-1)\hat{\gamma}}, & \text{if } q > 1, \end{cases} \tag{40}$$

where we recall here that q is the total number of independent terms that consist of DBC γ_n, and $\hat{\gamma}$ is the average power at the RN. With the proper substitutions and calculations, the probability of error for GSM (20), in terms of SER, results in

1) for $q = 1$

$$\begin{aligned}
\mathrm{P}_s^{\mathrm{GSM}} \leq -\frac{N_1}{2P}\int_0^\infty &\left(\frac{1}{3}\exp\left(-\frac{\gamma_n}{2}\right) + \exp\left(-\frac{2\gamma_n}{3}\right)\right) \\
&\times \ln\frac{2\gamma_n}{P}d\gamma_n = \frac{a + b\ln P^{-1}}{P},
\end{aligned} \tag{41}$$

where a, b are numerical values resulting from the calculation of the integral. With the proper calculations the diversity order follows as

$$\begin{aligned}
d_{\mathrm{GSM}} &= \lim_{P\to\infty} -\frac{\log \mathrm{P}_s^{\mathrm{GSM}}}{\log P} \\
&= \lim_{P\to\infty}\left(-\frac{\log\left(a + b\ln P^{-1}\right)}{\log P} + \frac{\log P}{\log P}\right) = 1.
\end{aligned} \tag{42}$$

2) for $q > 1$

$$\begin{aligned}
\mathrm{P}_s^{\mathrm{GSM}} \leq &\frac{N_1}{2(q-1)P} \\
&\times \int_0^\infty\left(\frac{1}{3}\exp\left(-\frac{\gamma_n}{2}\right) + \exp\left(-\frac{2\gamma_n}{3}\right)\right)d\gamma_n \\
&= a_1 P^{-1},
\end{aligned} \tag{43}$$

where a_1 is a numerical value resulting from the calculation of the integral. With the proper substitutions and calculations the diversity order follows as

$$\begin{aligned}
d_{\mathrm{GSM}} &= \lim_{P\to\infty} -\frac{\log \mathrm{P}_s^{\mathrm{GSM}}}{\log P} \\
&= \lim_{P\to\infty}\left(-\frac{\log a_1}{\log P} + \frac{\log P}{\log P}\right) = 1.
\end{aligned} \tag{44}$$

For the simplified case of SM technique, the result of diversity order is identical to GSM and equal to one. Specifically for the case of GSMA technique, the same methodology as in GSM is followed. With the proper substitutions and calculations, the probability of error for GSMA (23), in terms of SER, results in

1) $q = 1$, both for γ_1 and γ_2

$$\mathrm{P}_s^{\mathrm{GSMA}} \leq \frac{(a_1 + b_1\ln P^{-1})(a_2 + b_2\ln P^{-1})}{P^2}, \tag{45}$$

2) $q = 1$, for γ_1 and $q > 1$, for γ_2 and vice versa

$$\mathrm{P}_s^{\mathrm{GSMA}} \leq \frac{(a_1 + b_1\ln P^{-1})a_3}{P^2}, \tag{46}$$

3) $q > 1$,both for γ_1 and γ_2

$$\mathrm{P}_s^{\mathrm{GSMA}} \leq \frac{a_4}{P^2} \tag{47}$$

where $a_1, a_2, a_3, a_4, b_1, b_2$ are numerical values resulting from the calculation of the integrals, in each case. With the proper substitutions and calculations the diversity order results in

$$d_{\mathrm{GSMA}} = \lim_{P\to\infty} -\frac{\log \mathrm{P}_s^{\mathrm{GSMA}}}{\log P} = 2. \tag{48}$$

Hence the expression of Proposition 3 is derived.

REFERENCES

[1] O. Vermesan et al., "Internet of Things strategic research roadmap," in *Internet of Things Global Technological and Societal Trends From Smart Environments and Spaces to Green ICT*, River, 2011, pp. 9–52.

[2] A. Al-Fuqaha, M. Guizani, M. Mohammadi, M. Aledhari, and M. Ayyash ,"Internet of things: A survey on enabling technologies, protocols and applications," *IEEE Commun. Surveys Tutorials* , Vol. 17, no. 4, pp. 234776, Nov. 2015.

[3] K. Han and K. Huang, "Wirelessly powered backscatter communication networks: Modeling, coverage, and capacity," *IEEE Trans. Wireless Commun.*, vol. 16, Apr. 2017.

[4] M. Palattella, M. Dohler, A. Grieco, G. Rizzo, J. Torsner, T. Engel and L. Ladid, "Internet of things in the 5G era: Enablers, architecture and business models," *IEEE J. Selected Areas Commun.* , Vol. 34, no. 3, pp. 51027, Mar. 2016.

[5] H. Ding, J. Han, A. X. Liu, W. Xi, J. Zhao, P. Yang, and Z. Jiang, "Counting human objects using backscatter radio frequency signals," *IEEE Trans. on Mob. Comp.*, vol. 18, pp. 1054–1067, Jul. 2018.

[6] E. Moradi, S. Amendola, T. Bjorninen, L. Sydanheimo, J. M. Carmena, J. M. Rabaey, and L. Ukkonen, "Backscattering neural tags for wireless brain-machine interface systems," *IEEE Trans. on Ant. and Prop.*, vol. 63, pp. 719–726, Dec. 2014.

[7] S. Daskalakis, G. Goussetis, S. D. Assimonis, M. M. Tentzeris, and A. Georgiadis, "A uW backscatter-Morse-leaf sensor for low-power agricultural wireless sensor networks," *IEEE Sensors Journal*, vol. 18, pp. 7889–7898, Jul. 2018.

[8] F. Pereira, H. Sampaio, R. Chaves, R. Correia, M. Lus, S. Sargento, M. Jordo, L. Almeida, C. Senna, A. S. R. Oliveira, and N. B. Carvalho, "When backscatter communication meets vehicular networks: boosting crosswalk awareness," *IEEE Access*, vol. 8, pp. 34507–34521, Feb. 2020.

[9] B. Ji, B. Xing, K. Song, C. Li, H. Wen, and L. Yang, "The efficient BackFi transmission design in ambient backscatter communication systems for IoT," *IEEE Access*, vol. 7, pp. 31397–31408, Feb. 2019.

[10] N. V. Huynh, D. T. Hoang, X. Lu, D. Niyato, P. Wang, D. I. Kim, "Ambient backscatter communications: A contemporary survey," *IEEE Commun. Surveys Tut.*, vol. 20, pp. 2889–2922, May 2018.

[11] S. Thomas, and M. Reynolds, "A 96 mbit/sec, 15.5 pj/bit 16-qam modulator for UHF backscatter communication," *IEEE Int. Conf. RFID*, pp. 185–190, Orlando, USA, 2012.

[12] C. Boyer, and S. Roy, "Communication and RFID: Coding, Energy, and MIMO Analysis," *IEEE Trans. Commun.*, vol. 62, pp. 770–785, Dec. 2013.

[13] Y. Alsaba, S. K. A. Rahim, and C. Y. Leow, "Beamforming in wireless energy harvesting communications systems: A survey," *IEEE Commun. Surveys Tuts.*, vol. 20, pp. 1329–1360, 2018.

[14] K.V.S. Rao, P.V. Nikitin and S.F. Lam, "Antenna design for UHF RFID tags: a review and a practical application," in *IEEE Trans. Antenna Propag.*, vol.53, pp. 3870–3876, 2005.

[15] C. Xu, Le.Yang, and P. Zhang, "Practical backscatter communication systems for battery-free Internet of Things," *IEEE Commun. Surveys Tuts.*, vol. 35, pp. 16–27, Sep. 2018.

[16] G. Wang, F. Gao, R. Fan and C. Tellambura, "Ambient backscatter communication systems: Detection and performance Analysis," *IEEE Trans. Commun.*, vol. 64, pp. 4836–4846, Nov. 2016.

[17] P. Alevizos, A. Bletsas, and G. N. Karystinos, "Noncoherent short packet detection and decoding for scatter radio sensor networking," *IEEE Trans. Commun.*, vol. 65, pp. 21282140, May 2017.

[18] W. S. Lee, C. H. Kang, Y. K. Moon, and H. K. Song, "Determination scheme for detection thresholds using multiple antennas in Wi-Fi backscatter systems," *IEEE Access*, vol. 5, pp. 22159–22165, 2017.

[19] J. Qian, F. Gao, G. Wang, S. Jin, and H. Zhu, "Noncoherent detections for ambient backscatter system," *IEEE Trans. Wireless Commun.*, vol. 16, pp. 1412–1422, Mar. 2017.

[20] J. Griffin and G. Durgin, "Gains for RF tags using multiple antennas," *IEEE Trans. Antennas Propag.*, vol. 56, pp. 563–570, Feb. 2008.

[21] C. Hen, X. Chen, Z.J. Wang and W. Su, "On the performance of MIMO RFID backscattering channels," *EURASIP J. Wireless Commun. Net.*, pp. 1–15, Nov. 2012.

[22] C. He, H. Luan, X. Li, C. Ma, L. Han, and Z. J. Wang, "A simple, high-performance space-time code for MIMO backscatter communications," *IEEE Internet of Things Journal (Early Access)*, Feb. 2020.

[23] M. G. Livadaru, and J. L. Volakis, "Fabrication and measurements of a low-cost, dual-polarized advanced planar array with wide scanning coverage," *IEEE Inter. Sympos. on ANtn. and Prop. and USNV/URSI Nation. Radio Scien. Meet.*, Oct. 2017.

[24] M. B. Akbar, M. M. Morys, C. R. Valenta, and G. D. Durgin, "Range improvement of backscatter radio systems at 5.8 GHz using tags with multiple antennas," *Proc. of the 2012 IEEE Intern. Symp. on Ant. and Prop.*, Nov. 2012.

[25] A. Younis, N. Serafimovski, R. Mesleh and H. Haas, "Generalised spatial modulation," in *Conf. Rec. Asilomar Conf. Signals, Syst., Comput.*, Pacific Grove, CA, pp. 1498–1502, Nov. 2010.

[26] J. Jeganathan, A. Ghrayeb and L. Szczecinski, "Spatial modulation: Optimal detection and performance analysis," *IEEE Commun. Letters*, vol. 12, Aug. 2008.

[27] R. Mesleh, H. Haas, S. Sinanovic, C. W. Ahn and S. Yun, "Spatial modulation," *IEEE Trans. Veh. Technol.*, vol. 57, pp. 2228–2241, Jul. 2008.

[28] E. Basar, U. Aygolu, E. Panayirci and H. V. Poor, "Space-time block coded spatial modulation," *IEEE Trans. Commun.*, vol. 59, pp. 823–832, Mar. 2011.

[29] S. Alamouti, "A simple transmit diversity technique for wireless communications," *IEEE J. Sel. Areas Commun.*, vol. 16, Oct. 1998.

[30] Z. Niu, W. Wang and T. Jiang, "Spatial modulation for ambient backscatter communications: modeling and analysis," *IEEE Glob. Commun. Conf. (GLOBECOM)*, Waikoloa, HI, USA, Dec. 2019.

[31] Z. Ma, F. Gao, J. Jiang and Y.Liang, "Cooperative detection for ambient backscatter assisted generalized spatial modulation," *IEEE Glob. Commun. Conf. (GLOBECOM)*, Waikoloa, HI, USA, Dec. 2019.

[32] Y. Zhang, F. Gao, L. Fan, X. Lei, and G. K. Karagiannidis , "Secure communications for multi-tag backscatter systems," *IEEE Wirel. Comm. Lett.*, vol.8, pp.1146–1149, Aug. 2019.

[33] B. Zhu, J. Cheng, M. Alouini, and L. Wu, "Relay Placement for FSO multihop DF systems with link obstacles and infeasible regions," *IEEE Trans. on Wirel. Comm.*, vol.14, pp.5240–5250, Sep. 2015.

[34] M. Alkhawatrah, Y. Gong, G. Chen, S. Lambotharan, and J. A. Chambers, "Buffer-aided relay selection for cooperative NOMA in the internet of things," *IEEE Intern. of Thin. Journ.*, vol.6, pp.5722–5731, Jun. 2019.

[35] Q. Li, M. Wen, M. D. Renzo, H. V. Poor, S. Mumtaz, and F. Chen, "Dual-Hop spatial modulation with a relay transmitting its own information," *IEEE Trans. on Wirel. Commun. (Early Access)*, Apr. 2020.

[36] N. Fasarakis-Hilliard, P. N. Alevizos and A. Bletsas "Coherent Detection and Channel Coding for Bistatic Scatter Radio Sensor Networking," *IEEE Trans. Commun.*, vol. 63, pp. 1798–1810, May. 2015.

[37] D.Tse and P. Viswanath, *Fundamentals of Wireless Communications*, Cambridge University press, Aug. 2004.

[38] F. Fuschini, C. Piersanti, F. Paolazzi, and G. Falciasecca, "Analytical approach to the backscattering from UHF RFID transponder," *IEEE Antenna Wireless Propag. Lett.*, vol. 7, pp. 33–35, Feb. 2008.

[39] X. Guo and X.G. Xia, "On full diversity space-time block codes with partial interference cancellation group decoding," *IEEE Trans. Inf. Theory*, vol. 55, pp. 4366–4385, Oct. 2009.

[40] J. G. Proakis and M. Salehi, *Digital Communications*, McGraw-Hill, 5th ed., 1995.

[41] J. R. Hampton, *Introduction to MIMO Communications*, Cambridge University Press, 2014.

[42] Matlab and Optimization Toolbox User Guide, Release 2013, The MathWorks, Inc., Natick, Massachusetts, United States.

[43] C.M. Dardari, D. Simon, "New exponential bounds and approximations for the computation of error probability in fading channels," *IEEE Trans. Wireless Commun.*, vol. 4, pp. 840–845, Aug. 2008.

[44] M. Abramowitz, IA Stegun, *Handbook of Mathematical Functions*, National Bureau of Standards, Washington, DC, 1972.